RHIC PHYSICS*

C. Pajares

Departamento de Física de Partículas
Universidad de Santiago de Compostela
15706 Santiago de Compostela, Spain

(Received April 12, 1999)

A brief review of the hadronic phase transitions is presented by emphasizing the physical ideas and the main signatures of the transition in relation to the most significant results of the SPS experiments and the description of the RHIC experiments.

PACS numbers: 11.80.La, 12.38.Mh, 13.75.Cs

1. Introduction

The new incoming experiments RHIC have originated great expectation, due to the opportunity of studying nuclear matter under abnormal conditions of very high density and temperature. The interest on the subject comes from the seventies [1, 2]. More recently the SPS data already anticipated some results which have not explanation under conventional Physics. Here, it is presented a brief overview for non experts on the field, where due to space-time limitations some details are excluded. We will first have a look at the physical concepts which led to the idea that matter at sufficiently high density will undergo a transition to a state of deconfined quarks and gluons, and then we will turn to the results of statistical QCD related to the deconfined and/or chiral symmetry restoration phase transition. Also the main signatures of collective effects in high energy nucleus–nucleus collisions and the main unconventional results of SPS will be presented. Finally, we will show the four RHIC detectors and their goals in relation with the investigation of the collective effects.

* Presented at the XXVII International Meeting on Fundamental Physics, Sierra Nevada, Granada, Spain, February 1–5, 1999.

2. The colour screening in dense matter and the vacuum QCD

An increase of the energy density of a pion gas leads not only to the production of more pions, but also to abundant resonance production. The partition function of an ideal resonance gas is

$$\log Z = \frac{VT^3}{\pi^2} \int dm\rho(m)\mathrm{e}^{-\frac{m}{T}}, \tag{2.1}$$

where $\rho(m)$ is the resonance mass spectrum. In general, to determine $\rho(m)$ we need to know the hadron dynamics. In the statistical bootstrap model [3], the resonances are composed of resonances, giving rise to

$$\rho(m) \sim m^a \mathrm{e}^{bm}, \tag{2.2}$$

where b is fixed by the lowest hadron mass, m_π, and thus, $b \simeq 150$ MeV. The dual resonance model assumes the interaction amplitude to be built up by resonances in all channels [4], leading also to the same form of equation (2.2). Now, b is determined by the slope α' of the Regge-trajectories governing the spin degeneracy of resonances, and the resulting value is similar to that obtained by the statistical bootstrap model. Let us mention that the dual resonance model has an underlying string structure whose tension is fixed by the slope α'. The same form (2) was had previously been obtained from geometrical arguments [5], b was fixed through the size of the basic hadrons, leading again to a value close to 150 MeV.

Inserting (2) into (1), the integral diverges for $T > T_\mathrm{c} \equiv 1/b$. What is the meaning of the temperature T_c? An ultimate temperature T_c was proposed long time ago by Hagedorn [3]. In order to reach T_c the parameter a must be such that the energy density $\varepsilon \to \infty$. Later, it was noted [6] that for slightly smaller a values, ε remains finite and only higher derivatives of the partition function diverge, suggesting a phase transition.

These considerations lead to the question of what happens to colour confinement in such a transition.

The mechanism responsible for colour deconfinement is charge screening in a dense medium. The Coulomb potential between two electric charges changes in a dense ionized gas due to Debye screening

$$\frac{e^2}{r} \to \left(\frac{e^2}{r}\right) \mathrm{e}^{-\mu_D r}, \tag{2.3}$$

with a screening radius $r_D = 1/\mu_D$. In a similar way, the colour potential changes due to colour charges screening

$$\sigma r \to \left(\frac{1 - \mathrm{e}^{-\mu r}}{\mu r}\right) \sigma r, \tag{2.4}$$

where $1/\mu$ is the colour screening radius. With increasing colour charge density, μ increases and the bound state is dissolved [7] as it is shown in Fig. 1.

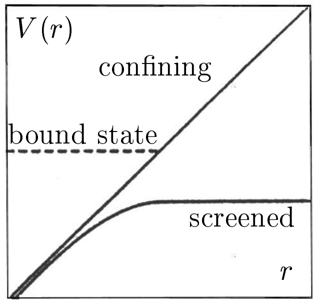

Fig. 1. Effect of screening on a confining potential

Thus, at low density we have a colour insulator: hadronic matter is just colour neutral bound quark states. At high density we have a colour conductor whose constituents are unbound coloured quarks and gluons.

We should note that the situation is different to the confinement of magnetic charges. That is, if one breaks a bar magnet in two, each half becomes a complete magnet with one positive and one negative poles, so to get a magnetic monopole is not possible. In the usual description, a magnetic monopole is considered either a fictitious invisible object or a real object but with a very heavy mass and therefore not yet seen. On the contrary, the quarks are believed to be real objects of relatively low masses, and, furthermore their interaction becomes very weak at high energies.

The QED–QCD analogy can be as follows: The QCD vacuum is considered as a condensate of gluon pairs and quark–antiquarks pairs so that it is a perfect colour dia-electric (colour dielectric constant $\chi = 0$). This is in analogy to electron pairs of a superconductor in BCS theory, which results in making the superconductor a perfect dia-magnet (magnetic susceptibility $\mu = 0$). Changing from QED to QCD we replace the magnetic field H by the colour electric field E, the superconductor by the QCD vacuum and the QED vacuum by the interior of the hadron (in the QED vacuum $\mu = 1$, and inside the hadron $\chi = 1$). The roles of the inside and the outside are intercharged. Just as the magnetic field is expelled outward from the semiconductor, the colour electric field is pushed into the hadron by the QCD vacuum, and that leads to colour confinement [8]. The situation can be seen in Fig. 2. The product of the colour dielectric times the colour magnetic susceptibility of the QCD vacuum is one, so since the QCD vacuum is a perfect colour dia-electric, its colour magnetic susceptibility is infinite.

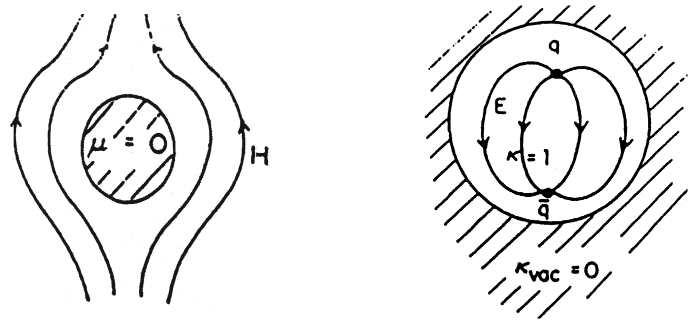

$\mu_{\rm vac} = 1$

Superconductor = Perfect Diamagnet **QCD Vacuum = Perfect Color Dia-electric**

Fig. 2. Superconductivity in QED *vs.* quark confinement in QCD

Computing the partition function for a free gas

$$\log Z(T,\mu,V) \; = \; \frac{gV}{6\pi^2 T}\int\limits_0^\infty \frac{dKK^4}{\sqrt{K^2+m^2}}\left[\frac{1}{\exp\{\left[\sqrt{K^2+m^2}-\mu\right]/T\}+\eta} + \frac{1}{\exp\{\left[\sqrt{K^2+m^2}+\mu\right]/T\}+\eta}\right], \tag{2.5}$$

where $\eta = +1(-1)$ for fermions (bosons), μ is the chemical potential and g the number of freedom degrees. Equation (5) leads for massless fermions ($m=0$) and bosons ($m=0, \mu=0$), respectively to

$$\begin{aligned} (T\log Z)_f \; &= \; \frac{g_t V}{12}\left(\frac{7}{30}\pi^2 T^4 + \mu^2 T^2 + \frac{\mu^4}{2\pi^2}\right), \\ (T\log Z)_b \; &= \; \frac{g_b V}{90}\pi^2 T^4 \, . \end{aligned} \tag{2.6}$$

Adding the negative term due to the constant vacuum pressure B, the partition function of a gas of quarks and gluons is given by

$$(T\log Z)_{\rm QGP} = \frac{N_{\rm c}N_f V}{6}\left(\frac{7\pi^2T^4}{30} + \mu_Q^2 T^2 + \frac{\mu_Q^4}{2\pi^2}\right) + \frac{\pi^2}{45}N_g V T^4 - BV, \tag{2.7}$$

where $N_{\rm c}$, N_f and N_g are the colour, flavour and gluon numbers, and $\mu_Q = 1/3\mu$. In the same way we can write the partition function for a pion gas.

The phase equilibrium of the pion gas and the Quark Gluon Plasma (QGP) is obtained by setting equal pressure for both phases

$$P = \frac{T}{V} \log Z. \tag{2.8}$$

For reasonable values of B, $B^{\frac{1}{4}} \simeq 0.150$ GeV, and $N_c = 3$, $N_f = 2$. The phase diagram is like the one in Fig. 3. This phase diagram could be more complicated due to the chiral symmetry restoration phase transition. Also, it has been pointed out that it should appear a tricritical point joining different phases [9].

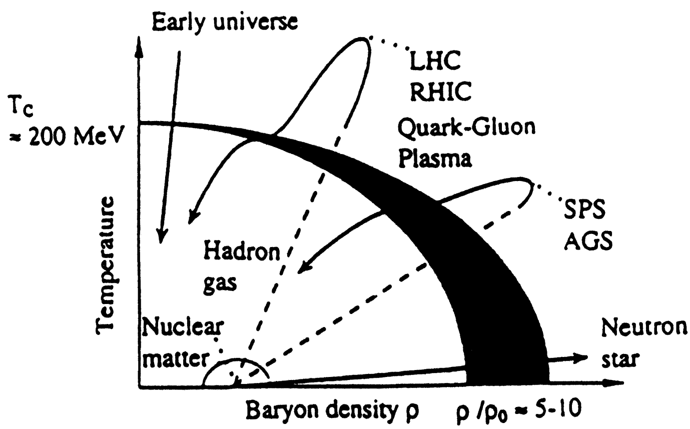

Fig. 3. The phase diagram of strongly interacting matter, showing the hadronic phase at low temperature and baryon density, the transition region (mixed phase) and the QGP phase. The full curves lines illustrate trajectories followed in supernovae explosions, Big Bang evolution, and possibly in heavy-ion reactions at present and future accelerators.

Coming back to the diagram in Fig. 3, at high temperature and at very low baryon number $(B/\gamma) \sim 10^{-10}$ it is the cosmic phase transition from the original Quark Gluon Plasma to hadronic matter which took place when the universe was 10^{-4}s–10^{-5}s old. Also, the possible locations of the possible transitions in heavy ion collisions for the different accelerators for normal nuclear matter and for neutral stars are shown. Other possible stable objects like stranglets [77] are not shown because it would be necessary an additional axis for the strangeness degree of freedom.

Long time ago, it was pointed out [10] the possibility of percolation of the hadronic particles produced in a heavy ion collision due to the overlapping of the sizes of such particles at high densities. The 3-D percolation threshold dimensionless parameter, η_C, it would be related to the density of particles n_C with radius r by the equation

$$\eta_C = \frac{4}{3}\pi r^3 n_C\,. \tag{2.9}$$

However, the universal value of $\eta_C = 0.34$, for $r = 0.8$–1 fm gives rise to a very low critical density, even below the density of normal nuclear matter.

This nonsense result can be overcame by realizing [11] that the first objects which are formed in a heavy ion collision are strings which decay in particles later on. These strings are formed between partons of the projectile and the target, having a transversal size that corresponds to a radius $r_0 \simeq 0.2$ fm. For a given nucleus–nucleus collision at fixed impact parameter, the strings can be seen as circles of area πr_0^2 inside the total available area (for a central, $b = 0$, A–A collision this area is πR_A^2). These circles overlap each other forming clusters of strings. The percolation of strings takes place when one path of overlapping circles through the available area appears, see Fig. 4. The dimensionless parameter threshold of this 2-D percolation is given by [11]

$$\eta_C = \pi r_0^2 n_C\,, \tag{2.10}$$

where n_C is the density of strings which depends on the profile function nuclei, and the value of η_C is in the range 1.12–1.5, corresponding to a value of n_C, $n_C \simeq 8.9$–11.9 strings/fm^2. At SPS energies even Pb–Pb collisions at $b = 0$ are below this threshold, while at RHIC energies will be above the threshold.

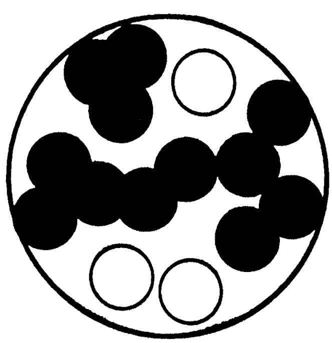

Fig. 4. Percolation of strings in transverse plane

3. Statistical QCD

The main results from the computer simulation of lattice QCD for $\mu = 0$ are summarized [12] in Fig. 5 and 6. In Fig. 5, the deconfinement measure $\langle L \rangle$ and the chiral condensate $\langle \bar{\Psi}\Psi \rangle/(4T)^3$ which are, respectively, the order parameters of the confinement and of the chiral symmetry restoration phase transitions, are plotted. The Polyakov loop, $\langle L \rangle$, can be related to the potential $V(r)$ between a static quark and antiquark in the limit of the infinite separation

$$\langle L \rangle \sim \lim_{r\to\infty} \exp(-V(r)/T). \tag{3.1}$$

For a confined state, $V(r)$ diverges for $r \to \infty$, so that $\langle L \rangle = 0$. In a deconfined state, $V(r)$ remains finite as $r \to \infty$, since colour screening cuts out the diverging behaviour and, hence, it confines the long distance component of the potential. In Fig. 5, the abrupt changes in $\langle L \rangle$ and $\langle \bar{\Psi}\Psi \rangle$ are seen at the same critical temperature $T_{\rm c} \sim 150$ MeV, showing that for $\mu = 0$ the two critical phenomena coincide.

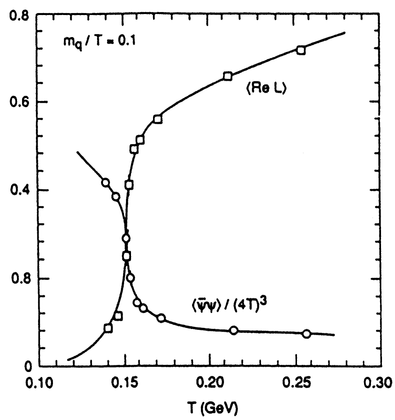

Fig. 5.

In Fig. 6, we see that at $T \sim T_{\rm c}$ the dimensionless energy density ε/T^4 increases from a value near that of an ideal pion gas (~ 1) to one similar to that of an ideal QGP. The increase in the energy density, $\Delta\varepsilon$, is the latent heat of the phase transition. We also observe that the ideal gas relation $\varepsilon = 3P$ is not fulfilled in the region $T_{\rm c} \leq T \leq 2T_{\rm c}$. Therefore, in this region there are definite interactions effects.

Such a value of $T_{\rm c}$ means that an energy density of around 1 GeV/fm^3 is needed to reach deconfinement. Is there a sufficient energy density at accelerator energy to reach this energy density? According to Bjorken [13], for A–A collisions the two nuclei can be seen as two Lorentz pancakes with

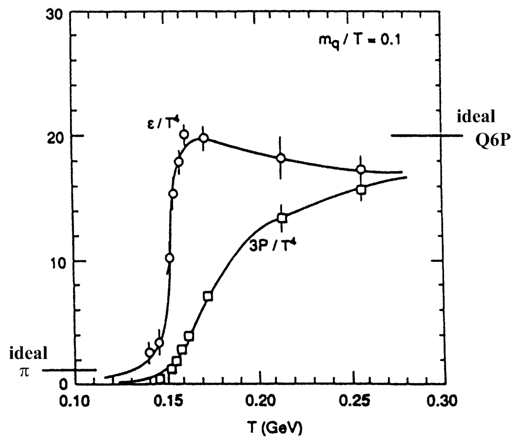

Fig. 6.

the energy

$$E \simeq \sqrt{\langle p_{\mathrm{T}} \rangle^2 + m_\pi^2}\ \frac{dN_\pi}{dy} \tag{3.2}$$

concentrated in the volume

$$V = \pi R^2 L\,, \qquad\qquad L = c r_0\,, \tag{3.3}$$

during the time of the collision ($r_0 \sim$ 1–2 fm) (see Fig. 7).

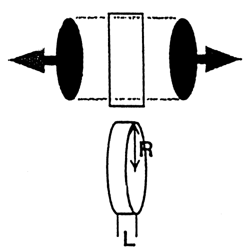

Fig. 7.

The ratio of (3.2) over (3.3) gives rise to the values of ε for the energies of the different accelerators which are plotted in Fig. 8. This evaluation of ε is optimistic. Indeed, the A–A collision can be considered as an incoherent superposition of many elementary collisions, in such a way that the energy is dissipated in a larger volume that (3.3), and therefore the energy density would be less than the obtained from (3.2) and (3.3).

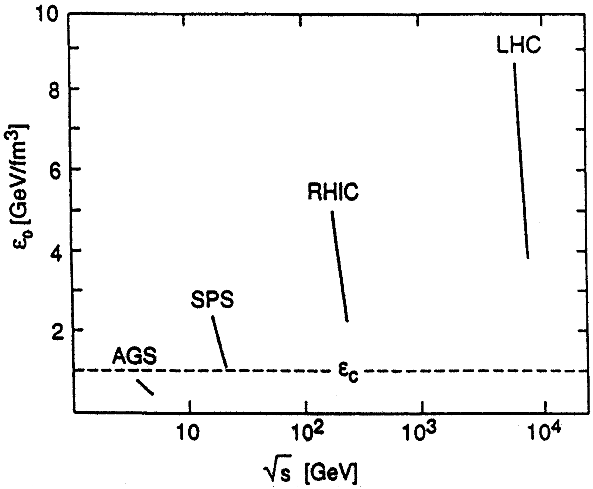

Fig. 8.

4. Signatures

A remarkable wealth of ideas has been put forward to determine how the experimental identification of the QGP could be accomplished. Most of the QGP signatures are not unambiguous and they can be explained by other kind of conventional and/or unconventional Physics. Probably, a clear proof of the detection of QGP should involve several combined signatures. Here, we discuss briefly some of the most relevant proposed signals.

4.1. Strangeness enhancement

The most frequently proposed signature for the restoration of spontaneously broken chiral symmetry in dense baryon rich hadronic matter are the enhancements in strangeness, antibaryon and heavy flavour production. The basic argument is the lowering of the thresholds for the production of heavy flavour hadrons and baryon–antibaryon pairs. An optimal signal is obtained by considering strange antibaryons which combine both effects [14]. The experimental data from SPS have shown strongly enhanced yields of Λ, $\bar{\Lambda}$, $\bar{\Xi}$, and Ω^-, $\bar{\Omega}^-$ hyperons [15]. However, such enhancements can be explained at least partially by other phenomena like gluon junction mechanism [16], colour rope [17], or string fusion [18].

Strangeness enhancement may also affect the ϕ-meson channel [19]. This was indeed observed at SPS energies [20]. Again, color rope or string fusion [21] can explain at least partially this enhancement.

4.2. Disoriented Chiral Condensates (DCC)

A direct signal for the restoration of chiral symmetry could come from DCC domains [22–24]. These correspond to isospin singlet, coherent excitations of the pion field, and would decay into neutral and charged pions with the probability distribution

$$P\left(\frac{N_{\pi^0}}{N_\pi}\right) \sim \frac{1}{2}\sqrt{\frac{N_\pi}{N_{\pi^0}}}. \tag{4.1}$$

Although the average ratio is $\langle N_{\pi^0}/N_\pi\rangle = 1/3$, as required by isospin symmetry, final states with a large surplus of charged pions over neutral pions, as than observed in Centauro [25] events, would occur with significant probability.

4.3. Quarkonium suppression

The suppression of J/ψ and ψ' are based on the insight that a bound state $c\bar{c}$ pair can not exist when the Debye colour screening length is less than the bound state radius [26]. Thus, a $c\bar{c}$ pair formed by fusion of two gluons from the colliding nuclei can not bind inside the QGP. To get bound, the $c\bar{c}$ pair has to escape of this region before the $c\bar{c}$ pair has been spatially separated by more than the size of the bound state. Therefore, if QGP is formed J/ψ and ψ' suppression is expected.

In the early 87, the NA38 collaboration [27] reported a J/ψ suppression in O–U and S–U collisions, but these data can be explained by absorption of the J/ψ, using a rather large "J/ψ"-N cross section of 6–7 mb [28, 29]. The "J/ψ" means a preasympotic state, not necessarily the $c\bar{c}$ bound state.

In 1996, the NA50 collaboration reported [30] an abnormal J/ψ suppression in Pb–Pb collisions, much stronger than the one expected due to absorption in very central collisions. Whether or not this effect can be totally explained by interaction with comovers [31,32], even in the case of very central collisions is an extensively discussed question.

4.4. Lepton pairs

Although they do not constitute proofs of the QGP lepton pairs from hadronic sources in the invariant mass range between 0.5 and 1 GeV could be valuable signals of the dense hadronic matter formed in nuclear collisions. The suggestion [33] that the disappearance of the ρ-meson peak in the lepton pair mass spectrum would signal a deconfining transition has recently been revived [34]. The widths and positions of the ρ, ω and ϕ peaks are also sensitive to induced changes in the hadronic mass spectrum [35, 36], especially to precursor phenomena associated with chiral symmetry restoration. A change in the K-meson mass also would affect the width of the ϕ-meson [37]. Some of these effects can be the responsible [38] for the excess of dielectrons seen by CERES collaboration in S–Au and Pb–Au collisions [39].

4.5. Direct high $p_{\rm T}$ photons

A hadron gas and a QGP near the critical temperature, $T_{\rm c}$, emits photon spectra of roughly equal intensity and similar spectral shape [40]. However, a clear signal of photons from the QGP would be visible for $p_{\rm T}$ in the range of 2–5 GeV/c if a very hot QGP is formed [41].

4.6. Behaviour of average $p_{\rm T}$ on multiplicity

In principle, one can invert the energy-temperature diagram of Fig. 6 to plot $\langle p_{\rm T}\rangle$ as a function of dN/dy, by assuming that $\langle p_{\rm T}\rangle$ measures the temperature and the multiplicity distribution on rapidity is proportional to the energy density. When a rapid change in the effective number of degrees of freedom occurs one expects that after a first rise of $\langle p_{\rm T}\rangle$, saturation arises due to the mixed phase [42, 43]. Finally, a second rise is expected. This behaviour, however, is not easy to disentangle from those given by another phenomena, like the normal QCD rise of $\langle p_{\rm T}\rangle$ with the energy, or the rise due to another effects like string fusion or percolation.

4.7. Transverse flow

In the presence of collective coherent effects there will be a collective transverse expansion and flow at midrapidity in relativistic heavy ion collisions [44]. Flow of baryons and mesons has been experimentally observed at AGS [45] and SPS in Pb–Pb collisions [46–48]. However, the observed transverse momentum of the different hadrons, and in particular the increase of the average $\langle p_{\rm T}\rangle$ with hadron mass, can be due to the secondary meson baryon collisions [48]. Recently [49], it has been shown that the magnitude of the elliptic flow is a good signal of a first order QGP phase transition.

4.8. Soft photons

It was proposed [50, 51] that parts of the QCD shower extend very far into the infrared domain and produce globs of ultrasoft partons. The matter in such an ultrasoft glob can be described as a cold QGP of sizeable parton number density, but very low energy per parton. This QGP would extend over rather large spatial volume with $R_{\rm T} \sim$ 4–6 fm. Bremsstrahlung emitted in collisions of partons in such QGP would dominate over the one from the initial and final state hadrons. The dependence of the rate of soft photons on the multiplicity could distinguish the collective behaviour from more conventional explanations [52, 53].

4.9. Intermittency

As the resolution of any variable of the phase space of multiparticle production decreases, the normalized momenta of the multiplicity distribution can diverge

$$\frac{\langle n(n-1)\dots n-(q+1)\rangle}{\langle n\rangle^q} \simeq (\delta y)^{-f_q}, \qquad f_q > 0. \tag{4.2}$$

The intermittent behaviour expressed by equation (4.4) can be originated by very different phenomena [54]. In particular, a phase transition like QGP produces intermittent behaviour with a determined dependence of the critical exponent, f_q, on q [55]. Also the type of the phase transition gives rise to different absolute values [56]. The dependence of f_q on the multiplicity can also help in the search of the QGP [55].

4.10. Cumulative effect

In some collective effects, like string fusion [57] or percolation of strings [11], clusters of strings are formed in such a way that the energy-momentum of the cluster is the sum of the energy-momentum of the original strings. The fragmentation of such clusters can produce particles outside the nucleon–nucleon kinematical limits because of their energy-momentum larger than the energy-momentum of a nucleon–nucleon collision. Experimentally, some $\bar{p}$ outside these limits were reported at Quark Matter 96 Conference in Heidelberg by the NA52 collaboration [58], but these data have not been confirmed [59].

4.11. Event by event fluctuations

Event by event studies can provide valuable dynamical information, in particular, departures from the superposition of independent nucleon–nucleon collisions can be detected by looking at the fluctuations on the average transverse momentum [60], strangeness [61] and particle number [62]. In this way collective effects could also be identified.

4.12. Long range correlations and forward backward correlations

Some collective effects like percolation of strings originate a typical behaviour of the long range correlations in rapidity [11,63]. Close to the critical point these correlations increase fast, decreasing again once the critical point is over. This behaviour can be detected by looking at the average multiplicity of particles produced in a backward rapidity interval, $\langle n_B \rangle$, as a function of the particles produced in a forward rapidity interval, n_F.

$$\langle n_B \rangle = a + b n_F \,, \tag{4.3}$$

$$b \equiv \frac{\langle n_B n_F \rangle - \langle n_B \rangle \langle n_F \rangle}{\langle n_F^2 \rangle - \langle n_F \rangle^2} \,. \tag{4.4}$$

The parameter b measures the long range correlations. The short range correlations are eliminated choosing the backward and forward intervals separated by 1.5–2 units of rapidity.

4.13. Enhancement of η production

The partial restoration of the axial U(1) symmetry of QCD and the related decrease of the η mass in regions of hot and dense matter should manifest itself in the increased production of η mesons [64, 65]. Also the increase of the yield of η mesons can create a hole in the low p_{T} region of the effective intercept parameter of the two-pion Bose–Einstein interference [66].

4.14. Jet quenching

It has been predicted [67] that close to the critical temperature the suppression of high p_{T} jets (jet quenching) due to the energy loss of partons will be reduced. Several studies show that jet $p_\perp$ broadening and induced energy loss may be significantly enhanced in hot matter as compared to cold matter [68, 69].

4.15. Bose–Einstein interference

The existence of dense droplets of QGP increases the probability of two hadrons being emitted very close to each other in coordinate space [70]. If the two hadrons are identical, Bose–Einstein interference will be magnified by the existence of droplets.

4.16. Cosmic-ray shower development

The most relevant parameter in the air shower development is the depth of maximum, $X_{\max}$. At the same collision energy, heavier elements develop faster in the atmosphere and produce shorter $X_{\max}$. In several cosmic ray experiments a rapid change on the slope of the $X_{\max}$ versus energy has been observed in the energy region 10^{17}–10^{18} eV. This change is usually interpreted as a change on the cosmic ray composition, from heavy to light elements. An alternative and natural explanation is the change on the dynamics of multiparticle production. In fact, collective effects like colour rope, string fusion [71], or percolation of strings [72] produce a reduction of the multiplicity in nucleus–air collisions, and, therefore, an increase of X_{max}. Precisely for central collisions of the heavy cosmic ray component, like Fe against Air, the threshold of percolation is reached around the above energies.

As we mentioned above, already SPS data have shown some signals which have not a clear conventional explanation, namely: The J/ψ suppression, the dilepton spectrum and the Λ, $\bar{\Lambda}$, Ξ, $\bar{\Xi}$, Ω^-, $\bar{\Omega}^-$ enhancements. This makes more exciting the search for collective effects in RHIC and LHC.

5. RHIC detectors

In RHIC there are two large experiments: STAR and PHENIX. Each experiment is participated by more than 40 institutions and near 400 people. Pictures of both detectors are shown in Fig. 9.

The philosophy of STAR [73] is to try to cover as large solid angle as possible. A clear advantage of this approach is that p_{T} distributions of particles, as well as two particles correlations, can be measured for one event. In this way, an event by event analysis becomes possible. A second advantage of this experiment is that a detailed reconstruction of each track is also possible, so that it will provide an useful tool for measuring V-particles such as Λ. Even though the capacity of particle identification is very limited, STAR will be a powerful tool to look at jets with $p_{\mathrm{T}} \geq 10$, 20 GeV$/c$, event by event fluctuations, F–B correlations and particle spectra for a large variety of particles, including strange baryons.

PHENIX [74] sets a strong emphasis on particle identification by covering a limited solid angle. Two arm spectrometers are prepared with tracking devices, RICH, TOF and EM calorimeters, to measure electrons, photons and identified hadrons. An event multiplicity will be measured by Si-strid and pad chambers over a rapidity region $-2.7 < y < 2.7$. PHENIX will study the yields of J/ψ, ψ', γ via leptonic channels, the ϕ and ω mesons via dielectron with mass resolution < 4 MeV, and via KK with mass resolution < 1 MeV. Also, it will study the photon radiation and the dependence of the average p_{T} of different hadrons on the multiplicity.

In addition to these large experiments there are two other interesting detectors: PHOBOS and BRAHMS.

PHOBOS [75] will be able to detect charged particles and photons in the range $-5.74 < \eta < 5.74$ and $0 \leq \phi \leq 2\pi$, and momentum of charged particles in the range $0 \leq \eta \leq 1.75$. A spectrometer is used to identify particle species by measuring their energy loss. PHOBOS detect very low

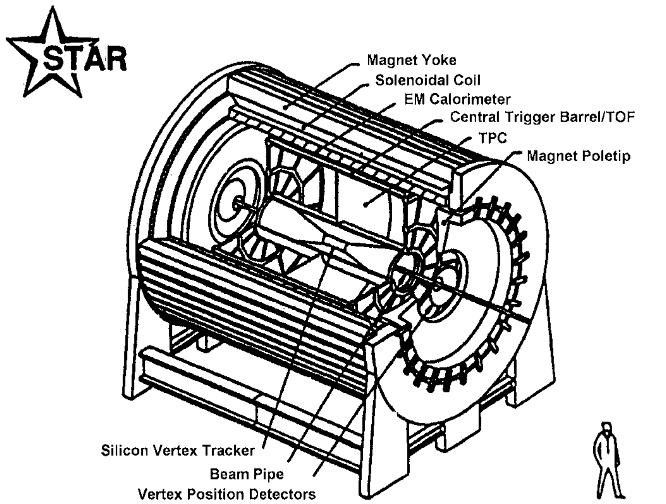

PHENIX DETECTOR

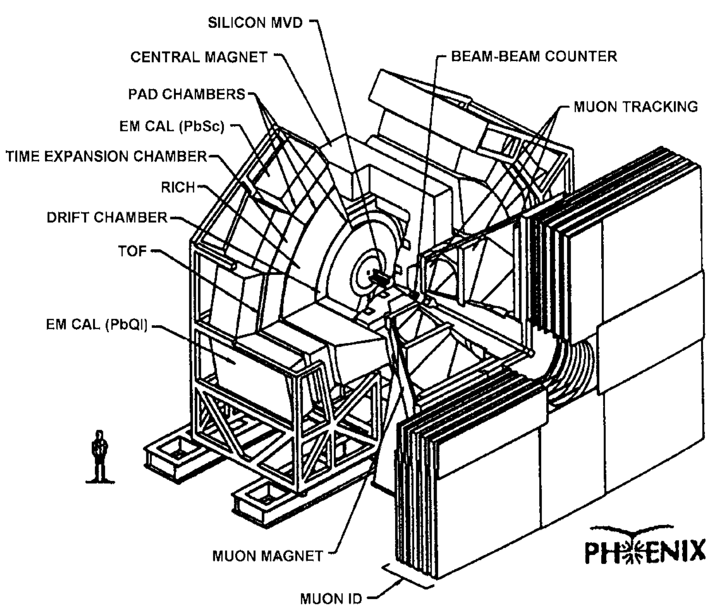

Fig. 9. Two large experiments, STAR (upper figure) and PHENIX (lower figure).

p_T, 20 MeV/c for π, 50 for K and 70 for p and $\bar{p}$. In this way, it will be very useful to search for $\pi^0/\pi^+ + \pi^-$ event by event, B–E interference, correlations, ϕ mass and width and so on.

BRAHMS [76] contains one forward and one mid-rapidity spectrometers. The first one has four magnets for sweeping and analyzing primary particles emerging from the reaction. Two arm tracking elements (small time projection chamber), one Cherenkov tank, complementary drift chambers for tracking determination, TOF and one RICH. The mid-rapidity spectrometer is designed to control the centrality of the collision, by measuring the multiplicity at central rapidity simultaneously to the forward particle production. It will be able to measure inclusive and semiinclusive $\pi^{\pm}$, $K^{\pm}$, p and $\bar{p}$ spectra at the fragmentation region. In this sense, the data from this detector can be very interesting, since the reached energies at RHIC and LHC are of the order of 10^{15}–10^{18} eV, overlapping with cosmic-ray information (remember that cosmic-ray shower are produced only in the fragmentation region).

6. Conclusions

The projected experiments in heavy-ion collisions will test the matter under abnormal conditions of pressure and temperature, which never have been explored before. Already, the SPS experiments are telling us that new physical unconventional phenomena could be at work. Sure enough, the RHIC and LHC experiments will provide us with surprises and a deeper knowledge of QCD.

This work was supported by CICYT of SPAIN under project AEN96-1673. I thank Prof. F. del Aguila and Prof. F. Cornet for organizing such a nice meeting, and Dr. C. Merino for a critical reading of the manuscript.

REFERENCES

[1] T.D. Lee, G.C. Wick, *Phys. Rev.* **D9**, 2291 (1974).

[2] J.C. Collins, M.J. Perry, *Phys. Rev. Lett.* **34**, 1353 (1975).

[3] R. Hagedorn, *Nuovo Cim. Suppl.* **3**, 147 (1965).

[4] G. Veneziano, *Nuovo Cim.* **57A**, 190 (1968); S. Fubini, G. Veneziano, *Nuovo Cim.* **A64**, 811 (1969); K. Bardakci, S. Mandelstam, *Phys. Rev.* 1640 (1969).

[5] I. Pomeranchuk, *Doklad. Akad. Nauk. SSSR* **78**, 889 (1951).

[6] N. Cabbibo, G. Parisi, *Phys. Lett.* **B59**, 67 (1975).

[7] H. Satz, *Proc. XXIV Int. Symposium on Multiparticle Dynamics*, eds. A. Giovannini *et al.*, World Scientific 1994.

[8] T.D. Lee at Quark Matter 95 Monterey, *Nucl. Phys.* **A590**, 11c (1995).

[9] R. Pisarski, F. Wilczek, *Phys. Rev.* **D29**, 338 (1984); M. Alford, K. Rajagopal, F. Wilczek, *Nucl. Phys.* **B537**, 443 (1999).

[10] G. Baym, *Physica* **96A**, 131 (1979); T. Celik, F. Karsch, H. Satz, *Phys. Lett.* **B97**, 128 (1980).

[11] N. Armesto, M.A. Braun, E.G. Ferreiro, C. Pajares, *Phys. Rev. Lett.* **77**, 3736 (1996); M.A. Braun, C. Pajares, J. Ranft, *Int. J. Mod. Phys.* **A** (to appear); M. Nardi, H. Satz, *Phys. Lett.* **B442**, 14 (1998); H. Satz, *Nucl. Phys.* **A642**, 130c (1998).

[12] T. Blum, L. Kärkkäinen, D. Toussaint, S. Gottlieb, XIIth International Symposium on Lattice Gauge Theory (Lattice 94), Bielefeld 1994.

[13] J.D. Bjorken, *Phys. Rev.* **D27**, 140 (1983).

[14] J. Rafelski, B. Müller, *Phys. Rev. Lett.* **48**, 1066 (1982); J. Rafelski, *Phys. Rep.* **88**, 331 (1982).

[15] WA97 Collaboration, E. Andersen *et al., Phys. Lett.* **B443**, 209 (1998); NA49 Collaboration, H. Appelshauser *et al., Phys. Lett.* **B444**, 523 (1998); WA85 Collaboration, F. Antinori *et al., Phys. Lett.* **B447**, 178 (1999).

[16] A. Capella, E.G. Ferreiro, C.A. Salgado, Orsay preprint LPTHE 99106 (1999); S.E. Vance, M. Gyulassy, X.N. Wang, *Phys. Lett.* **443B**, 45 (1998); A. Capella, B.Z. Kopeliovich, *Phys. Lett.* **381B**, 325 (1996).

[17] H. Sorge, M. Berenguer, H. Stöcker, W. Greiner, *Phys. Lett.* **289B**, 6 (1992).

[18] E.G. Ferreiro, C. Pajares, D. Sousa, *Phys. Lett.* **422B**, 314 (1997).

[19] A. Shor, *Phys. Rev. Lett.* **54**, 1122 (1985).

[20] NA38 Collaboration, C. Baglin *et al., Phys. Lett.* **272B**, 449 (1991).

[21] M. Berenguer, H. Stocker, W. Greiner, *Phys. Lett.* **332B**, 15 (19994); N. Armesto, M.A. Braun, E.G. Ferreiro, C. Pajares, *Phys. Lett.* **344B**, 301 (1995).

[22] A.A. Anselm, M.G. Ryskyn, *Phys. Lett.* **266B**, 482 (1989).

[23] J.P. Blaizot, A. Krzywicki, *Phys. Rev.* **D46**, 246 (1992).

[24] J.D. Bjorken, *Acta Phys. Pol.* **B23**, 637 (1992).

[25] C.M.G. Lattes, Y. Fujimoto, S. Hasegawa, *Phys. Rep.* **65**, 151 (1980).

[26] T. Matsui, H. Satz, *Phys. Lett.* **178B**, 416 (1986).

[27] NA38 Collaboration, C. Baglin *et al., Phys. Lett.* **B262**, 36 (1991).

[28] A. Capella, J.A. Casado, C. Pajares, A.V. Ramallo, J. Tran Thanh Van, *Phys. Lett.* **B206**, 354 (1988); A. Capella, C. Merino, J. Tran Thanh Van, C. Pajares, A.V. Ramallo, *Phys. Lett.* **B243**, 144 (1990).

[29] C. Gerschel, J. Hüfner, *Phys. Lett.* **B207**, 253 (1988) and *Z. Phys.* **C56**, 171 (1992).

[30] NA50 Collaboration, M.C. Abreu *et al., Phys. Lett.* **B410**, 327 (1997) and **B410**, 337 (1997).

[31] J.P. Blaizot, J.Y. Ollitrault, *Phys. Rev. Lett.* **77**, 1703 (1996); C.Y. Wong, *Phys. Rev.* **C55**, 2621 (1997); D. Kharzeev, C. Lourenco, M. Nardi, H. Satz, *Z. Phys.* **C74**, 307 (1997); R. Vogt, *Phys. Lett.* **B430**, 15 (1998).

[32] N. Armesto, A. Capella, E.G. Ferreiro, *Phys. Rev.* **C59**, 395 (1999); J. Geiss, C. Greiner, E.L. Brotkovskaya, W. Cassing, V. Morel, *Phys. Lett.* **B441**, 31 (1999).

[33] J.P. Siemens, S.A. Chin, *Phys. Rev. Lett.* **55**, 1266 (1985).

[34] D. Siebert, *Phys. Rev. Lett.* **68**, 1476 (1992).

[35] H.W. Barz, G. Bertsch, B.L. Friman, H. Schulz, S. Boggs, *Phys. Lett.* **B265**, 219 (1991).

[36] C.M. Ko, P. Levai, W.J. Qiu, *Phys. Rev.* **C46**, 1159 (1992).

[37] D. Lissauer, E.V. Shuryak, *Phys. Lett.* **B253**, 15 (1991).

[38] G.E. Brown, M. Rho, *Phys. Rev. Lett.* **66**, 2720 (1991); G.Q. Li, C.M. Ko, G.E. Brown, *Phys. Rev. Lett.* **75**, 4007 (1995).

[39] CERES Collaboration, G. Agakichiev *et al.*, *Phys. Rev. Lett.* **75**, 1272 (1995); *Phys. Lett.* **B422**, 405 (1998).

[40] J. Kapusta, P. Lichard, D. Seibert, *Phys. Rev.* **D44**, 2774 (1991); *Phys. Rev.* **D47**, 4171 (1993).

[41] S. Raha, B. Sinha, *Phys. Rev. Lett.* **58**, 101 (1987); D.K. Srivastava, B. Sinha, M. Gyulassy, X.M. Wang, *Phys. Lett.* **B276**, 285 (1992).

[42] L. Van Hove, *Phys. Lett.* **B118**, 138 (1982); *Z. Phys.* **C21**, 93 (1983).

[43] E.V. Shuryak, O. Zhirov, *Phys. Lett.* **B171**, 99 (1986).

[44] W. Scheid, H. Müller, W. Greiner, *Phys. Rev. Lett.* **32**, 741 (1974).

[45] E877 Collaboration, J. Barrete *et al.*, *Phys. Rev.* **C56**, 3254 (1997).

[46] NA44 Collaboration, I.G. Bearden *et al.*, *Phys. Rev. Lett.* **78**, 2080 (1997).

[47] NA49 Collaboration, P.G. Jones *et al.*, *Nucl. Phys.* **A610**, 188c (1996).

[48] WA98 Collaboration, T. Peitzmann *et al., Nucl.Phys.* **A638**, 415c (1998).

[49] H. Sorge, *Phys. Rev. Lett.* **82**, 2048 (1999).

[50] L. Van Hove, *Ann. Phys.* **192**, 66 (1989) and CERN preprint TH-5749 (1990).

[51] P. Lichard, L. Van Hove, CERN preprint TH-5747 (1990).

[52] M.I. Gorestein, O.P. Pavlenko, *Z. Phys.* **C37**, 611 (1988).

[53] M.G. Ryskin, *Phys. Lett.* **B209**, 529 (1988).

[54] A. Bialas, R. Peschanski, *Nucl. Phys.* **B273**, 703 (1986); *Phys. Lett.* **B207**, 59 (1988).

[55] A. Bialas, R. Hwa, *Phys. Lett.* **B253**, 436 (1991).

[56] R. Hwa, *Mod. Phys. Lett.* **A9**, 863 (1994); *Phys. Rev.* **D57**, 1831 (1998).

[57] N. Armesto, M.A. Braun, E.G. Ferreiro, C. Pajares, Yu.M. Shabelski, *Astropart. Phys.* **6**, 329 (1997); E.G. Ferreiro, C. Pajares, *Nucl. Phys.* (Proc. Suppl.) **B71**, 313 (1999).

[58] NA52 Collaboration, R. Klingerberg *et al.*, *Nucl. Phys.* **A610**, 306C (1996).

[59] NA52 Collaboration, *J. Phys. G* **25**, 225 and 217 (1999).

[60] M. Gazdzicki, S. Mrowczynski, *Z. Phys.* **C54**, 127 (1992); N. Armesto, M.A. Braun, E.G. Ferreiro, C. Pajares, *Z. Phys.* **C67**, 489 (1995); M. Gazdzicki, A. Leonidov, G. Roland, *Eur. Phys. J.* **C6**, 365 (1999) and hep-ph/9711422.

[61] L. Stodolsky, *Phys. Rev. Lett.* **75**, 1044 (1995).

[62] E.V. Shuryak, *Phys. Lett.* **B423**, 9 (1998).

[63] N. Amelin, N. Armesto, M.A. Braun, E.G. Ferreiro, C. Pajares, *Phys. Rev. Lett.* **73**, 2813 (1994).

[64] J. Kapusta, D. Kharzeev, L. McLerran, *Phys. Rev.* **D53**, 5028 (1996).

[65] Z. Huang, X.M. Wang, *Phys. Rev.* **D53**, 5054 (1996).

[66] S.E. Vance, T. Csörgo, D. Kharzeev, *Phys. Rev. Lett.* **81**, 2205 (1998).

[67] M. Gyulassy, M. Plumer, *Phys. Lett.* **B243**, 432 (1990); M. Gyulassy, X.M. Wang, *Nucl. Phys.* **B420**, 583 (1994); M. Gyulassy, X.M. Wang, M. Plumer, *Phys. Rev.* **D51**, 3236 (1995).

[68] R. Baier, Yu.L. Dokshitzer, S. Peigné, D. Shiff, *Phys. Lett.* **B345**, 277 (1995).

[69] A.H. Mueller, *Nucl. Phys.* **A610**, 459c (1996).

[70] S. Pratt, A. Vischer, P.J. Siemens, *Phys. Rev. Lett.* **68**, 1109 (1992).

[71] N. Armesto, M.A. Braun, E.G. Ferreiro, C. Pajares, Yu.M. Shabelski, *Phys. Lett.* **B389**, 78 (1996).

[72] C. Pajares, D. Sousa, R.A. Vázquez, Int. Symp. on Ultrahigh Energy Cosmic Ray, Gran Sasso, *Nucl. Phys.* **B** (Proc. Suppl.), to appear.

[73] J.W. Harris, *Nucl. Phys.* **A566**, 277c (1994).

[74] S. Nagamiya, *Nucl. Phys.* **A566**, 287c (1994).

[75] F. Wystouch, *Nucl. Phys.* **A566**, 287c (1994).

[76] F. Videboek, *Nucl. Phys.* **A566**, 301c (1994).

[77] E. Witten, *Phys. Rev.* **D30**, 272 (1984); A. de Rújula, S. Glashow, *Nature* **312**, 734 (1984); J.D. Bjorken, L.D. McLerran, *Phys. Rev.* **D20**, 2353 (1979).